2021 43rd Annual International Conference of the
IEEE Engineering in Medicine & Biology Society (EMBC)
Oct 31 - Nov 4, 2021. Virtual Conference

Transitive Inverse Consistent Rigid Longitudinal Registration of Diffusion Weighted Magnetic Resonance Imaging: A Case Study in Athletes With Repetitive Non-Concussive Head Injuries

Harshkumar S. Prajapati[1], Kian Merchant-Borna[2], Jeffrey J. Bazarian[2],
Cristian A. Linte[1,3], and Nathan D. Cahill[1,4]

Abstract— **Significant longitudinal changes in metrics derived from diffusion weighted magnetic resonance (MR) images of the brain have been observed in athletes subject to repetitive non-concussive head injuries (RHIs). Accurate alignment of longitudinal scans of a subject is an important step in detecting and quantifying these changes. Currently, tools such as DSI Studio [1], FreeSurfer [2], and FSL [3] perform pairwise rigid registration of all scans in a longitudinal sequence to the first time-point scan (or to another reference scan or template). While the rigid transformations obtained using this strategy can be computed in a manner that enforces inverse consistency, for the case of three or more scans, the transformations are not transitive. This can lead to discrepancy in the rigid transformations that can be measured in physical units. Using a diffusion MRI dataset collected and analyzed as part of a larger study in [4], [5], [6], we illustrate this discrepancy, and we show how it can lead to uncertainty in local/regional estimates of diffusion metrics including fractional anistropy (FA), mean diffusivity (MD), and quantitatve anisotropy (QA). Additionally, we propose a method to perform transitive longitudinal rigid registration of a sequence of scans in a manner that guarantees that the discrepancy in the transformations will be eliminated.**

Clinical relevance— **This paper establishes that standard processing pipelines for performing longitudinal analysis of diffusion MR images of the brain exhibit registration discrepancies that can be eliminated.**

I. INTRODUCTION

Diffusion-weighted magnetic resonance imaging (dMRI), also known as Diffusion-Weighted Imaging (DWI), is the most widely used imaging modality for studying the structural connectivity of the human brain, enabling investigations into the effects of disease on brain connectivity [7], [8], changes in structural connectivity during development and neurodegeneration [9], [10], [11], the organization of brain networks [12], [13], and the relationship between brain structure and function [14], [15]. Echo-planar images (EPIs) collected in DWI provide directional information about the diffusion of water molecules in the brain. In cerebral white matter (WM), water diffuses freely along the direction of fibers while being restricted in the transverse direction [16], [17]; hence, quantifying diffusion patterns enables inferring properties of WM structure.

Under the umbrella of DWI, Diffusion Tensor Imaging (DTI) fits local multivariate normal distributions to dewarped EPI data, generating a spatially varying field of tensors (covariance matrices) whose dominant eigenvectors can be interpreted as encoding local fiber directions [18], [19]. Quantitative indices like fractional anisotropy (FA) and mean diffusivity (MD) can be computed from each tensor, providing local information related to microstructure integrity and membrane density. One clinical example of where quantitative indices from DTI have yielded key insights is in athletes subjected to repetitive non-concussive head injuries (RHIs). Studies have shown that American football players subjected to RHIs experienced significant changes in FA and MD observed in images acquired over the course of a football season when compared to healthy controls [20]. Moreover, changes in FA from pre- to post-season were found to be positively correlated with several helmet impact measures (computed from helmet-mounted accelerometers) [4] and with declines in several neurocognitive measures [6]. These findings have been confirmed by others using DTI to examine RHIs in boxing [21], ice hockey [22], soccer [23], and American football [24].

These studies on RHIs have all investigated global longitudinal changes in indices derived from DTI. It would also be beneficial to investigate local and/or regional longitudinal changes in a subject if the longitudinal scans of that subject can be accurately aligned. Furthermore, if the scans of multiple subjects can be accurately registered to a template (e.g., MNI ICBM-152 [25]), local and/or regional inter-subject comparisons between longitudinal changes in FA, MD, or other DTI-derived indices can be performed. Freely available research software such as FSL [3], FreeSurfer [2], and DSI Studio [1] provide functionality that enables users to register scans according to rigid, affine, and/or locally deformable transformations.

DSI Studio in particular [1] has also emerged as a powerful tool for exploring more sophisticated reconstruction methods than DTI, including q-ball imaging (QBI) [26], diffusion

*This work was supported by grants from the National Institutes of Health (Award No. R35GM128877) and the National Science Foundation (Award No. OAC 1808530).

[1]Harshkumar S. Prajapati, Cristian A. Linte, and Nathan D. Cahill are with the Center for Imaging Science, Rochester Institute of Technology, Rochester, NY, USA {hsp1981,ndcsma,calbme}@rit.edu

[2]Kian Merchant-Borna and Jeffrey J. Bazarian are with Emergency Medicine Research, University of Rochester Medical Center, Rochester, NY, USA {Kian_Merchant-Borna, Jeff_Bazarian}@URMC.Rochester.edu

[3]Cristian A. Linte is with the Department of Biomedical Engineering, Rochester Institute of Technology, Rochester, NY, USA

[4]Nathan D. Cahill is with the School of Mathematical Sciences, Rochester Institute of Technology, Rochester, NY, USA

spectrum imaging (DSI) [27], generalized q-sampling imaging (GQI) [28], and q-space diffeomorphic reconstruction (QSDR) [29], all of which we consider as being under the umbrella of DWI. As opposed to using diffusion tensors, which are inadequate for resolving crossing or "kissing" fibers, these methods use spin distribution functions (SDFs) and/or orientation distribution functions (ODFs) to model local diffusion. This enables indices such as quantitative anisotropy (QA) to be computed locally in any desired direction, not just in a single dominant direction as in FA.

In many of the RHI studies that have explored indices derived from DTI, three or more longitudinal scans are available for each subject; for example, for one or more years, each subject may undergo a pre-season scan, an immediate post-season scan, and a scan after a post-season rest period. To perform intra-subject registration of a series of three or more scans, it is reasonable to assume that the scans differ geometrically by rigid transformations (notwithstanding the possibility of cerebral edema, growing tumors, etc.). Practically, DSI Studio, FreeSurfer, or FSL could be used to perform pairwise rigid registration of all scans to the first scan in the series (or to some other selected scan or template). However, such a strategy does not guarantee optimal registration across all scans in a series: even if the second and third scans are each optimally registered to the first scan, it is very likely that composing these transformations to create a mapping from the third scan to the second scan will yield a transformation that is inconsistent with the transformation found had the third scan been optimally registered directly to the second scan.

For three or more images, standard pipeline like DSI Studio is only set up to perform pairwise rigid registration. However, there are issues with transitivity of the rigid transformations. In this work, we show via experiments the practical impact of these issues (by measuring the discrepancy/inconsistency in terms of physical units). In addition, we also show the impact on the variability associated with several image-specific measures, including FA, MD, and QA.

Furthermore, in response to these findings, we propose a new method for simultaneous longitudinal rigid registration of three or more scans that guarantees that this discrepancy/inconsistency will be eliminated. As such, this proposed method will enable the extension of the original white matter integrity studies mentioned earlier.

II. PRELIMINARIES

Let $\{I_1, \ldots, I_n\}$ be a sequence of images defined (in physical coordinates) over $\mathbb{R}^3$, and define $g_{j,i} : \mathbb{R}^3 \to \mathbb{R}^3$, $g_{j,i}(\mathbf{x}) = \mathbf{R}^{(j,i)}\mathbf{x} + \mathbf{t}^{(j,i)}$, to be a rigid transformation with rotation matrix $\mathbf{R}^{(j,i)} \in \mathbb{R}^{3\times 3}$ and translation vector $\mathbf{t}^{(j,i)} \in \mathbb{R}^3$ that maps coordinates of I_j into coordinates of I_i. We denote $I_j^{g_{j,i}}$ to be the result of transforming the image I_j according to $g_{j,i}$; that is, $I_j^{g_{j,i}} : \mathbb{R}^3 \to \mathbb{R}$, $I_j^{g_{j,i}}(\mathbf{x}) = I_j(g_{j,i}(\mathbf{x}))$.

Suppose we have a set of regions $\{\Omega_1, \ldots, \Omega_n\}$ in $\mathbb{R}^3$ over which we observe $\{I_1, \ldots, I_n\}$, for example, corresponding to regions of brain tissue in DTI scans. If I_j is transformed according to $g_{j,i}$, the region Ω_j is transformed into $\Omega_j^{g_{j,i}} = \{g_{j,i}(\mathbf{x}) \,|\, \mathbf{x} \in \Omega_j\}$. To quantify the similarity between an image I_i and a transformed image $I_j^{g_{j,i}}$ over the intersections of their regions of interest, we define a cost function $C_{i,j}(g_{j,i}) = S(I_i, I_j, \Omega_i, \Omega_j, g_{j,i})$. The average similarity between all pairs of images in the sequence can then be defined by:

$$C(\mathcal{G}) = \frac{1}{n(n-1)} \sum_{i \neq j} C_{i,j}(g_{j,i}) \ , \tag{1}$$

where $\mathcal{G} = \{g_{i,j} \,|\, i = 1, \ldots n;\ j = 1, \ldots n;\ i \neq j\}$. In this paper, we define S to be the correlation coefficient between I_i and $I_j^{g_{j,i}}$ over $\Omega_i \cap \Omega_j^{g_{j,i}}$; however, S could be chosen to be any other similarity measure such as mutual information, correlation ratio, negative mean squared difference, etc.

There are two properties of the transformations in $\mathcal{G}$ that should be satisfied when longitudinal registration is performed:

- *Inverse consistency*: $g_{i,j} = g_{j,i}^{-1}$, $\forall i \neq j$.
- *Transitivity*: $g_{i,j} = g_{k,j} \circ g_{i,k}$, $\forall i \neq j \neq k$.

III. RELATED WORK

Over the years many methods have been proposed to handle the registration of three or more images in the groupwise setting. These methods have then been adopted to the longitudinal setting when longitudinal studies for longer duration became more common. One such approach is to create a template from the available images and register each image to that template. Joshi *et al.* [30] describe mathematically an optimal technique to determine this template such that each image requires minimal transformation. However, their technique does not satisfy inverse consistency or transitivity.

Woods *et al.* [31] proposed one of the earliest techniques to generate a transitive set transformations in groupwise rigid image registration. Their method performs a posthoc rectification of a set of pre-computed pairwise rigid transformations by defining a discrepancy measure which is minimized using Newton's method; however, it does not optimize any measure of image similarity in the rectification step. Gass *et al.* [32] proposed a technique to rectify precomputed pairwise non-rigid deformations that iteratively minimizes inconsistency between projections of gridpoints using linear least squares, generating a set of approximately transitive transformations. Christensen *et al.* [33] proposed a method for pairwise inverse consistent nonrigid registration by estimating forward and reverse transformations simultaneously and constraining them to be inverses of one another. However, this method does not address transitivity of a set of transformations. Geng *et al.* [34] perform nonrigid inverse consistent groupwise registration with respect to an implicit reference so as to avoid bias to a particular image.

The work most closely related to this paper is by Arganda-Carreras *et al.* [35], which proposes a nonrigid scheme for registering sequences of three images that is transitive and approximately inverse consistent. Here, we focus on the rigid registration case, enabling us to exactly satisfy both inverse

consistency and transitivity, and we illustrate a framework that is applicable to $n \geq 3$ images in a sequence.

IV. METHODS

A. Pairwise Rigid Registration

In longitudinal registration of n images of the same subject, the first image (I_1) is often used as a reference, and the subsequent images in the sequence are registered to the first image. This can be achieved by maximizing the corresponding $C_{1,j}$'s to determine the optimal estimates of $g_{j,1}$ for $j = 2, \ldots, n$. Each $\mathbf{R}^{(j,1)}$ can be parameterized in terms of its three Euler angles, for example, yielding a set of 6 parameters representing each $g_{j,1}$.

B. Inverse Consistent Pairwise Rigid Registration

In rigid registration, it is straightforward to ensure inverse consistency. If we define $g_{i,j}(\mathbf{x}) = \mathbf{R}^{(i,j)}\mathbf{x} + \mathbf{t}^{(i,j)}$ so that $\mathbf{R}^{(i,j)} = \left(\mathbf{R}^{(j,i)}\right)^{\mathbf{T}}$ and $\mathbf{t}^{(i,j)} = -\left(\mathbf{R}^{(j,i)}\right)^{\mathbf{T}}\mathbf{t}^{(j,i)}$, then $g_{i,j}$ and $g_{j,i}$ are exact inverses of one another.

Noting that (1) can be rewritten as:

$$C(\mathcal{G}) = \frac{1}{n(n-1)} \sum_{i<j} B_{i,j}(g_{j,i}) \ , \tag{2}$$

where $B_{i,j}(g_{j,i}) = C_{i,j}(g_{j,i}) + C_{j,i}(g_{i,j})$. Expressing both $g_{i,j}$ and $g_{j,i}$ in terms of $\mathbf{R}^{(j,i)}$ and $\mathbf{t}^{(j,i)}$ allows us to perform pairwise inverse consistent rigid registration by maximizing each of the $B_{i,j}$'s with respect to the 6 parameters in $g_{j,i}$.

C. Pairwise Rigid Registration Discrepancy

In pairwise rigid registration of a sequence of images (whether inverse consistent or not), the transformations obtained by maximizing the $C_{i,j}$'s or the $B_{i,j}$'s are not transitive. This means that the transformation $g_{i,j}$ that would be obtained by maximizing $C_{i,j}$ or $B_{i,j}$ is almost certainly different from the transformation $\widetilde{g}_{i,j}$ that would be obtained by composing the transformations $g_{j,k}^{-1}$ with $g_{i,k}$ relating I_i and I_j to any other image I_k.

This nontransitivity leads to a discrepancy between the position of $g_{i,j}(\mathbf{x})$ and $\widetilde{g}_{i,j}(\mathbf{x})$, which in some situations can be substantial. To quantify this discrepancy over a sequence of images, we first define the pointwise discrepancy for an image I_i at $\mathbf{x}$ with respect to images I_j and I_k as:

$$\eta_{i,j,k}(\mathbf{x}) = \left\| (g_{j,i} \circ g_{i,j})(\mathbf{x}) - (g_{j,i} \circ g_{k,j} \circ g_{i,k})(\mathbf{x}) \right\| \ , \tag{3}$$

where $\|\cdot\|$ is the Euclidean norm. The pointwise discrepancy values can be integrated over Ω_i to yield a discrepancy measure $\eta_{i,j,k}$ for an image I_i with respect to images I_j and I_k. We then define the total mean discrepancy η for the sequence of n images as:

$$\eta = \frac{1}{n(n-1)(n-2)} \sum_{i} \sum_{j \neq i} \sum_{k \neq i,j} \eta_{i,j,k} \ . \tag{4}$$

D. Transitive Inverse Consistent Rigid Registration

In general, the transformations in $\mathcal{G}$ are neither inverse consistent nor transitive. However, suppose we start with only a subset $\hat{\mathcal{G}} \in \mathcal{G}$ given by $\hat{\mathcal{G}} = \{g_{2,1}, \ldots, g_{n,1}\}$. The remaining transformations in $\mathcal{G}$ can be constructed from those in $\hat{\mathcal{G}}$ via:

$$g_{i,j} = \begin{cases} g_{j,i}^{-1}, & i = 1 \, , \\ g_{j,1}^{-1} \circ g_{i,1}, & i > 1 \, . \end{cases} \tag{5}$$

This construction guarantees both inverse consistency and transitivity of the transformations in $\mathcal{G}$. Therefore, by construction, the resulting transformations will have discrepancies $\eta_{i,j,k} = 0$ for all i, j, and k, and the total mean discrepancy will be $\eta = 0$.

This observation suggests a method for performing *transitive inverse consistent* rigid registration of a sequence of n images: by expressing $C(\mathcal{G})$ as $C\left(\mathcal{G}\left(\hat{\mathcal{G}}\right)\right)$ and defining $\mathcal{G}\left(\hat{\mathcal{G}}\right)$ according to (5), the cost function (2) can be maximized with respect to the $6(n-1)$ parameters of the rigid transformations in $\hat{\mathcal{G}}$.

V. CASE STUDY: ATHLETES WITH RHIs

A. Data

To investigate the importance of inverse consistency and transitivity in a longitudinal registration pipeline, we perform a secondary analysis of a diffusion MRI data set that was previously collected and analyzed by co-authors of this paper as part of a larger study [4], [5], [6]. Over the course of two football seasons, a total of 19 athletes from the University of Rochester football team were recruited, along with 5 non-athletes from the general student body as controls. For all subjects, diffusion MR images were acquired at baseline/preseason (T1), immediately post-season (T2), and six months post-season (T3). All the scans were acquired at the Rochester Center for Brain Imaging on a 3T Siemens TIM Trio scanner with a 32-channel head coil. Single shot echo planar imaging was used (SS-EPI; 60 diffusion directions, TR = 8900 ms, TE = 86 ms, b = 2000 s/mm^2, 70 slices for $2 \times 2 \times 2\,\text{mm}^3$ image resolution) with 10 non-diffusion weighted (b=0) volumes acquired throughout the acquisition sequence. Of the 24 subjects, we only analyzed the data from the 20 subjects that had a full set of scans available at T1, T2, and T3.

B. Pre-Processing and Registration

For each subject, the raw DWI images from each scan are processed using the pipeline shown in Fig. 1. First, eddy current correction and B_0-field inhomogeneity correction are performed. Next, the corrected DWI scans are registered using either pairwise rigid registration (branch A in Fig. 1) or transitive inverse consistent rigid registration (branch B in Fig. 1). The pairwise rigid registration can either be inverse consistent, yielding a set of transformations $\mathcal{G}^{(pw-ic)}$, or non-inverse consistent, yielding $\mathcal{G}^{(pw-nic)}$; the transitive inverse consistent rigid registration yields a set of transformations $\mathcal{G}^{(tr-ic)}$. With the resulting set of transformations from either

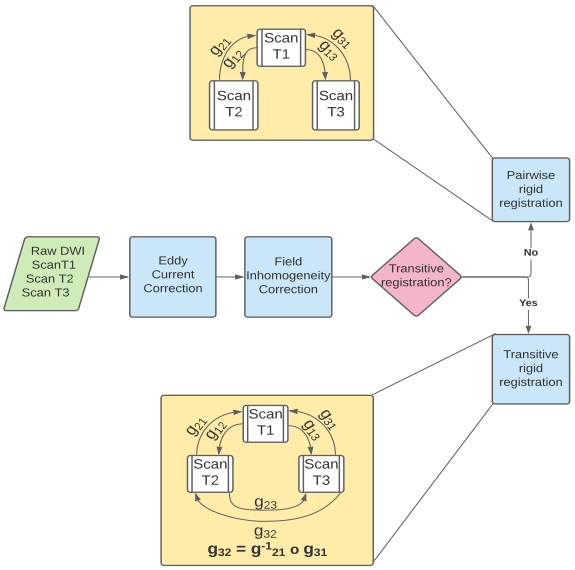

Fig. 1. Pre-Processing and Registration Pipeline

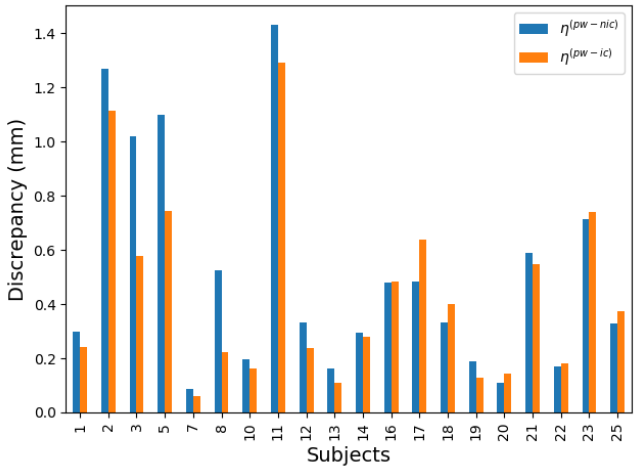

Fig. 2. Total mean discrepancy of pairwise rigid registration for each subject. Results show that total mean discrepancies of both inverse consistent (blue) and non-inverse consistent (orange) pairwise registration exceed 0.5 mm in six of the 20 subjects.

branch, all scans for a subject are transformed into the space of the subject's scan at time point T1.

C. Quantifying the Pairwise Registration Discrepancy

For each subject, we use both sets of pairwise rigid transformations ($\mathcal{G}^{(pw-nic)}$ and $\mathcal{G}^{(pw-ic)}$) to compute the total mean discrepancy η: for $\mathcal{G}^{(pw-nic)}$, we denote the total mean discrepancy $\eta^{(pw-nic)}$, and for $\mathcal{G}^{(pw-ic)}$, we denote it as $\eta^{(pw-ic)}$. As can be seen in Fig. 2, the average values of $\eta^{(pw-nic)}$ and $\eta^{(pw-ic)}$ across all subjects are: 0.51 mm and 0.43 mm, respectively. In six of the 20 subjects, both $\eta^{(pw-nic)}$ and $\eta^{(pw-ic)}$ exceed 0.5 mm, and in two of the subjects, both discrepancies exceed 1 mm. Given the nontrivial size of these discrepancies and the fact that they can be eliminated entirely through transitive registration, it will be useful to investigate the extent to which quantitative indices such as FA, MD, and QA differ when transitive registration versus nontransitive registration is performed in the processing pipeline.

To investigate whether it is possible that registration discrepancies can be influenced by the presence or absence of RHIs, we can compare discrepancies in athletes versus controls. Median $\eta^{(pw-nic)}$ values for athletes ($n_1 = 16$) and controls ($n_2 = 4$) are 0.330 and 0.714, respectively, and median $\eta^{(pw-ic)}$ values for athletes and controls are 0.326 and 0.490, respectively. We cannot reject the null hypotheses that the distributions of $\eta^{(pw-nic)}$ values are different in the two groups (Mann-Whitney $U = 25.0$, $p = 0.27$) and that the distributions of $\eta^{(pw-ic)}$ values are different in the two groups (Mann-Whitney $U = 27.0$, $p = 0.33$). In each case, we have $p > 0.05$, suggesting that there is not evidence to claim that the distributions of discrepancies differ in athletes and controls.

D. Local Diffusion Metrics

In the original studies using the data from these subjects [4], [5], [6], diffusion tensors were reconstructed from the corrected DWI scans, and diffusion metrics including FA and MD were computed from the tensors. In this paper, in order to investigate the *local* impact of discrepancies due to the non-transitivity of pairwise registration, we use DSI Studio [1] to perform a subsequent alignment step to register all of the longitudinal scans of each subject to the MNI template [36] prior to reconstructing diffusion tensors. Then, we extract FA and MD values from 48 anatomically relevant areas defined by the JHU DTI-based white matter atlas [37], [38]. DSI Studio enables this subsequent registration step in their implementation of QSDR reconstruction method [29], which reconstructs spin distribution functions (SDFs) as opposed to diffusion tensors. Hence, in addition to extracting FA and MD from diffusion tensors that are reconstructed in MNI space, we also extract QA values from the SDFs that are reconstructed via QSDR.

We use this procedure to extract FA, MD, and QA twice: a first time assuming that the longitudinal scans for each subject have been rigidly registered according to an inverse-consistent pairwise registration (yielding $\text{FA}^{(pw-ic)}$, $\text{MD}^{(pw-ic)}$, and $\text{QA}^{(pw-ic)}$), and a second time assuming that the longitudinal scans have been rigidly registered according to a transitive inverse-consistent registration (yielding $\text{FA}^{(tr-ic)}$, $\text{MD}^{(tr-ic)}$, and $\text{QA}^{(tr-ic)}$). For simplicity, we do not consider the case of pairwise non-inverse consistent registration of the longitudinal scans.

E. Impact of Pairwise Registration Discrepancies on FA, MD, and QA

For a particular diffusion metric (FA, MD, or QA), we denote the value of that metric at location $\mathbf{x}$ in scan i of subject j to be $\alpha_{i,j}(\mathbf{x})$. In each of the 48 regions

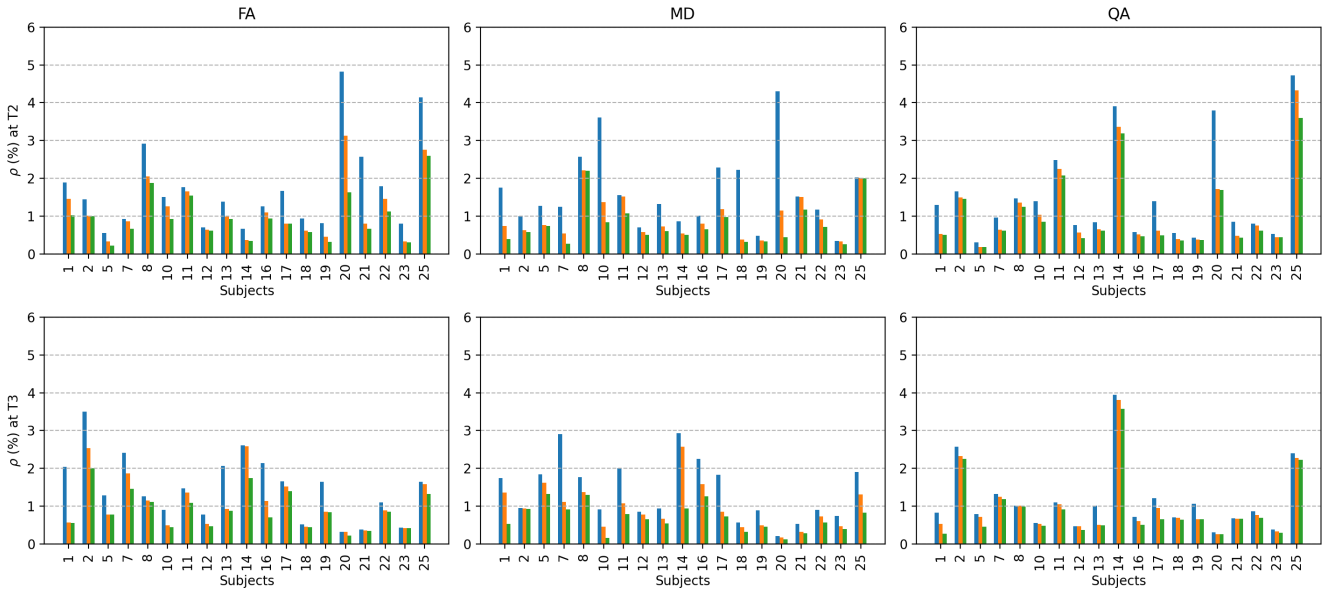

Fig. 3. Each subplot illustrates absolute differences in the mean values of the diffusion metric (FA, MD, QA) in specific regions, relative to the maximum possible value of the diffusion metric, arising from carrying out transitive longitudinal registration versus pairwise registration. Bars for each subject indicate the three largest differences out of the 48 regions in the JHU atlas.

defined by the JHU atlas, we compute the mean of the $\alpha_{i,j}$ values, yielding a set of sample means: $\mu_{i,j,1}$, $\mu_{i,j,2}$, ... , $\mu_{i,j,48}$. We then compute the absolute differences between the sample means, relative to the maximum possible value of the diffusion metric; i.e.,

$$\rho_{i,j,k} = \frac{\left| \mu_{i,j,k}^{(tr-ic)} - \mu_{i,j,k}^{(pw-ic)} \right|}{\nu_{i,j}} \cdot 100\% \ , \qquad (6)$$

for $k = 1, \ldots, 48$, and where the normalization factor is $\nu_{i,j} = 1$ for FA and QA and $\nu_{i,j} = \max_{\mathbf{x}} \alpha_{i,j}^{(pw-ic)}(\mathbf{x})$ for MD.

When averaged across all regions and all subjects, the absolute differences in FA, MD, and QA are 0.37%, 0.30%, and 0.57% of the maximum possible values, respectively, for T2 scans, and 0.32%, 0.20%, and 0.51% for T3 scans. Even though these average differences across all regions and subjects are fairly small, specific regions of particular subjects can exhibit substantially larger differences. Each subplot of Fig. 3 displays, for a particular diffusion metric and a particular time point (T2 or T3), the three regions for each subject (the three values of k) for which the values of $\rho_{i,j,k}$ are largest. Note that since both pairwise registration and transitive longitudinal registration are performed with the scan at time T1 as the reference scan, all values of $\rho_{i,j,k}$ are identically zero for the time T1 scans.

As can be seen from Fig. 3, for FA, MD, and QA, respectively, 6, 6, and 4 of the 20 subjects contain at least one brain region in at least one of the time points in which transitive versus non-transitive longitudinal registration yields absolute differences exceeding 2% relative to the maximum value of the diffusion metric. Further, subjects 20 and 25 contain regions where absolute differences in at-least one of the FA, MD and QA measures exceed 4% relative to the respective maximum values.

In the context of studying whether/how diffusion metrics change in athletes subjected to RHIs over the course of a football season, the use of standard pairwise rigid registration for a sequence of longitudinal scans may be suitable for studying global changes in these metrics due to relatively low average values of ρ. However, care should be taken when studying local/regional changes in diffusion metrics over time, given that the nontransitive nature of pairwise rigid registration can cause $2\% - 4\%$ differences (or more) in some regions of particular subjects versus the values of the metrics that would be found in those regions when transitive longitudinal registration is performed.

VI. Conclusion

In this paper, we noted that standard pairwise rigid registration algorithms that are often used in assessing longitudinal changes in diffusion weighted MR brain images are nontransitive, leading to a registration discrepancy that can be eliminated by performing transitive rigid longitudinal registration. We subsequently proposed an algorithm for carrying out transitive rigid longitudinal registration. In the context of college athletes subjected to repetitive subconcussive head impacts over the course of a football season, we showed that the average registration discrepancy that arises from standard processing pipelines can exceed 1 mm in many subjects. Furthermore, we show that this discrepancy leads to local / regional differences in diffusion metrics such as FA, MD, and QA, that can exceed 2% (and up to 4% or more) of their maximum possible values.

Based on these results, we recommend that studies of longitudinal changes in diffusion weighted MR images employ

transitive rigid longitudinal registration as opposed to pairwise rigid registration, especially when studies focus on local / regional changes. This guarantees that any discrepancy due to non-transitivity of the registration algorithm is eliminated, allowing greater confidence in assessing changes in diffusion metrics over time.

REFERENCES

[1] "DSI Studio," http://dsi-studio.labsolver.org.

[2] "FreeSurfer," http://surfer.nmr.mgh.harvard.edu/.

[3] M. Jenkinson, C. F. Beckmann, T. E. Behrens, M. W. Woolrich, and S. M. Smith, "FSL," *Neuroimage*, vol. 62, no. 2, pp. 782–790, 2012.

[4] J. J. Bazarian, T. Zhu, J. Zhong, D. Janigro, E. Rozen, A. Roberts, H. Javien, K. Merchant-Borna, B. Abar, and E. G. Blackman, "Persistent, long-term cerebral white matter changes after sports-related repetitive head impacts," *PLOS ONE*, vol. 9, no. 4, p. e94734, Apr 2014.

[5] K. Merchant-Borna, P. Asselin, D. Narayan, B. Abar, C. M. C. Jones, and J. J. Bazarian, "Novel method of weighting cumulative helmet impacts improves correlation with brain white matter changes after one football season of sub-concussive head blows," *Annals of Biomedical Engineering*, vol. 44, no. 12, p. 3679–3692, Dec 2016.

[6] M. C. Mayinger, K. Merchant-Borna, J. Hufschmidt, M. Muehlmann, I. R. Weir, B.-S. Rauchmann, M. E. Shenton, I. K. Koerte, and J. J. Bazarian, "White matter alterations in college football players: a longitudinal diffusion tensor imaging study," *Brain Imaging and Behavior*, vol. 12, no. 1, p. 44–53, Feb 2018.

[7] N. A. Crossley, A. Mechelli, J. Scott, F. Carletti, P. T. Fox, P. McGuire, and E. T. Bullmore, "The hubs of the human connectome are generally implicated in the anatomy of brain disorders," *Brain*, vol. 137, no. 8, p. 2382–2395, Aug 2014.

[8] A. Fornito, A. Zalesky, and M. Breakspear, "The connectomics of brain disorders," *Nature Reviews Neuroscience*, vol. 16, no. 33, p. 159–172, Mar 2015.

[9] D. S. Bassett, C. H. Xia, and T. D. Satterthwaite, "Understanding the emergence of neuropsychiatric disorders with network neuroscience," *Biological Psychiatry: Cognitive Neuroscience and Neuroimaging*, vol. 3, no. 9, p. 742–753, 2018.

[10] S. Oldham and A. Fornito, "The development of brain network hubs," *Developmental Cognitive Neuroscience*, vol. 36, p. 100607, 2019.

[11] T. Zhao, Y. Xu, and Y. He, "Graph theoretical modeling of baby brain networks," *NeuroImage*, vol. 185, p. 711–727, 2019.

[12] E. Bullmore and O. Sporns, "Complex brain networks: graph theoretical analysis of structural and functional systems," *Nature Reviews Neuroscience*, vol. 10, no. 3, p. 186–198, Mar 2009.

[13] M. P. van den Heuvel and O. Sporns, "Network hubs in the human brain," *Trends in Cognitive Sciences*, vol. 17, no. 12, pp. 683 – 696, 2013, special Issue: The Connectome. [Online]. Available: http://www.sciencedirect.com/science/article/pii/S1364661313002167

[14] C. J. Honey, J.-P. Thivierge, and O. Sporns, "Can structure predict function in the human brain?" *NeuroImage*, vol. 52, no. 3, p. 766–776, 2010.

[15] J. Goñi, M. P. v. d. Heuvel, A. Avena-Koenigsberger, N. V. d. Mendizabal, R. F. Betzel, A. Griffa, P. Hagmann, B. Corominas-Murtra, J.-P. Thiran, and O. Sporns, "Resting-brain functional connectivity predicted by analytic measures of network communication," *Proceedings of the National Academy of Sciences*, vol. 111, no. 2, p. 833–838, Jan 2014.

[16] P. Basser, J. Mattiello, and D. LeBihan, "Diagonal and off-diagonal components of the self-diffusion tensor: their relation to and estimation from the nmr spin-echo signal," *Proc. 11th Annu. Meet. SMRM, Berlin*, vol. 1, p. 1222, 1992.

[17] T. L. Chenevert, J. A. Brunberg, and J. G. Pipe, "Anisotropic diffusion in human white matter: Demonstration with MR techniques in vivo." *Radiology*, vol. 177, no. 2, p. 401–405, 1990.

[18] P. J. Basser, J. Mattiello, and D. Lebihan, "Estimation of the effective self-diffusion tensor from the NMR spin echo," *Journal of Magnetic Resonance, Series B*, vol. 103, no. 3, p. 247–254, Mar 1994.

[19] P. J. Basser, J. Mattiello, and D. LeBihan, "MR diffusion tensor spectroscopy and imaging." *Biophysical Journal*, vol. 66, no. 1, p. 259–267, Jan 1994.

[20] J. J. Bazarian, T. Zhu, B. Blyth, A. Borrino, and J. Zhong, "Subject-specific changes in brain white matter on diffusion tensor imaging after sports-related concussion," *Magnetic Resonance Imaging*, vol. 30, no. 2, pp. 171–180, 2012.

[21] L. Zhang, L. Heier, R. Zimmerman, B. Jordan, and A. Uluğ, "Diffusion anisotropy changes in the brains of professional boxers," *American Journal of Neuroradiology*, vol. 27, no. 9, pp. 2000–2004, 2006.

[22] I. K. Koerte, D. Kaufmann, E. Hartl, S. Bouix, O. Pasternak, M. Kubicki, A. Rauscher, D. K. Li, S. B. Dadachanji, J. A. Taunton *et al.*, "A prospective study of physician-observed concussion during a varsity university hockey season: White matter integrity in ice hockey players. Part 3 of 4," *Neurosurgical Focus*, vol. 33, no. 6, p. E3, 2012.

[23] I. K. Koerte, B. Ertl-Wagner, M. Reiser, R. Zafonte, and M. E. Shenton, "White matter integrity in the brains of professional soccer players without a symptomatic concussion," *Journal of the American Medical Association*, vol. 308, no. 18, pp. 1859–1861, 2012.

[24] T. W. McAllister, J. C. Ford, L. A. Flashman, A. Maerlender, R. M. Greenwald, J. G. Beckwith, R. P. Bolander, T. D. Tosteson, J. H. Turco, R. Raman *et al.*, "Effect of head impacts on diffusivity measures in a cohort of collegiate contact sport athletes," *Neurology*, vol. 82, no. 1, pp. 63–69, 2014.

[25] J. Mazziotta, A. Toga, A. Evans, P. Fox, J. Lancaster, K. Zilles, R. Woods, T. Paus, G. Simpson, B. Pike *et al.*, "A probabilistic atlas and reference system for the human brain: International Consortium for Brain Mapping (ICBM)," *Philosophical Transactions of the Royal Society of London. Series B: Biological Sciences*, vol. 356, no. 1412, pp. 1293–1322, 2001.

[26] D. S. Tuch, "Q-ball imaging," *Magnetic Resonance in Medicine*, vol. 52, no. 6, p. 1358–1372, Dec 2004.

[27] V. J. Wedeen, P. Hagmann, W.-Y. I. Tseng, T. G. Reese, and R. M. Weisskoff, "Mapping complex tissue architecture with diffusion spectrum magnetic resonance imaging," *Magnetic Resonance in Medicine*, vol. 54, no. 6, p. 1377–1386, Dec 2005.

[28] F.-C. Yeh, V. J. Wedeen, and W.-Y. I. Tseng, "Generalized q-sampling imaging," *IEEE transactions on medical imaging*, vol. 29, no. 9, p. 1626–1635, Sep 2010.

[29] F.-C. Yeh and W.-Y. I. Tseng, "NTU-90: a high angular resolution brain atlas constructed by q-space diffeomorphic reconstruction," *NeuroImage*, vol. 58, no. 1, p. 91–99, Sep 2011.

[30] S. Joshi, B. Davis, M. Jomier, and G. Gerig, "Unbiased diffeomorphic atlas construction for computational anatomy," *NeuroImage*, vol. 23, pp. S151–S160, 2004.

[31] R. P. Woods, S. T. Grafton, C. J. Holmes, S. R. Cherry, and J. C. Mazziotta, "Automated image registration: I. General methods and intrasubject, intramodality validation," *Journal of Computer Assisted Tomography*, vol. 22, no. 1, pp. 139–152, 1998.

[32] T. Gass, G. Székely, and O. Goksel, "Consistency-based rectification of nonrigid registrations," *Journal of Medical Imaging*, vol. 2, no. 1, p. 014005, Mar. 2015.

[33] G. E. Christensen and H. J. Johnson, "Consistent image registration," *IEEE Transactions on Medical Imaging*, vol. 20, no. 7, pp. 568–582, Jul. 2001.

[34] X. Geng, G. E. Christensen, H. Gu, T. J. Ross, and Y. Yang, "Implicit reference-based group-wise image registration and its application to structural and functional MRI," *NeuroImage*, vol. 47, no. 4, pp. 1341–1351, 2009.

[35] I. Arganda-Carreras, C. O. S. Sorzano, P. Thévenaz, A. Muñoz-Barrutia, J. Kybic, R. Marabini, J. M. Carazo, and C. Ortiz-de Solorzano, "Non-rigid consistent registration of 2D image sequences," *Physics in Medicine & Biology*, vol. 55, no. 20, p. 6215, 2010.

[36] F.-C. Yeh, S. Panesar, D. Fernandes, A. Meola, M. Yoshino, J. C. Fernandez-Miranda, J. M. Vettel, and T. Verstynen, "Population-averaged atlas of the macroscale human structural connectome and its network topology," *NeuroImage*, vol. 178, p. 57–68, Sep 2018.

[37] S. Mori, K. Oishi, H. Jiang, L. Jiang, X. Li, K. Akhter, K. Hua, A. V. Faria, A. Mahmood, R. Woods, and et al., "Stereotaxic white matter atlas based on diffusion tensor imaging in an icbm template," *NeuroImage*, vol. 40, no. 2, p. 570–582, Apr 2008.

[38] "Neurovault," https://identifiers.org/neurovault.collection:264.